Journal of Membrane Science 493 (2015) 524–538

Contents lists available at ScienceDirect

Journal of Membrane Science

journal homepage: www.elsevier.com/locate/memsci

Controlling molecular weight cut-off of PEEK nanofiltration membranes using a drying method

João da Silva Burgal, Ludmila Peeva, Patrizia Marchetti, Andrew Livingston *

Department of Chemical Engineering and Chemical Technology, Imperial College, Exhibition Road, London SW7 2AZ, UK

ARTICLE INFO

Article history:
Received 23 February 2015
Received in revised form
24 June 2015
Accepted 4 July 2015
Available online 8 July 2015

Keywords:
Poly(ether ether ketone)
Organic solvent nanofiltration
Drying method
Control of molecular weight cut-off
Statistical analysis

ABSTRACT

In this research paper we report two ways of controlling the molecular weight cut-off (MWCO) of PEEK membranes prepared via phase inversion and subsequent drying. The two methods explored were the change of polymer concentration in the dope solution – 8 wt%, 10 wt% and 12 wt% – and the variation of solvent filling the pores prior to drying – e.g. water, methanol, acetone, tetrahydrofuran and n-heptane. The results show that it is possible to vary the MWCO from 295 g mol^{-1} to 1400 g mol^{-1} by varying these parameters. A statistical analysis based on a genetic algorithm showed that the Hansen solubility parameter, polarity and their interactions with molar volume were likely to be the most important parameters influencing the performance of PEEK membranes when drying from different solvents. In addition, the drying temperature also proved to have an effect on the membrane performance – the higher the temperature the higher the rejection and the lower the permeance.

1. Introduction

Organic Solvent Nanofiltration (OSN) membranes can be used for separation in the chemical and pharmaceutical industry to perform concentration and purification and solvent recovery. Recently, it was shown how OSN could be used for catalytic reactions with reaction and separation occurring in situ under high temperature and basic conditions [1]. One of the main challenges of fabricating suitable OSN membranes is to have the right MWCO to perform the separation of interest. The most widely used method for manufacturing polymeric membranes is the phase inversion method. This method involves four mains steps: dissolving a polymer in an appropriate solvent (dope solution); membrane casting; phase inversion (wet or dry); and membrane post-treatment [2].

It is known that it is possible to manipulate the membrane performance by varying the composition of the dope solution, varying the conditions during the phase inversion step or via a post-treatment step (drying, conditioning or crosslinking) [3,4].

In the dope preparation step it is necessary to take into account the polymer concentration, the addition of volatile solvents, non-solvents (or 'bad' solvents) and pore forming additives [4]. It has been observed that polymer concentration has a significant effect on the viscosity which in turn affects the performance of the final membrane (higher concentration leads to higher selectivity but lower permeance) [5]. Volatile solvents such as ethylether (EE), tetrahydrofuran (THF) or dioxane, could be added to the dope solution in order to produce integrally skinned asymmetric membranes via the dry/wet method (where the evaporation step is essential) [6,7]. By allowing partial evaporation of the volatile solvent between the casting and immersion step, a skin-layer with elevated polymer concentration can be formed. Pore forming additives can be used to increase permeability and porosity with or without compromising the selectivity. For example addition of LiCl or $LiNO_3$ to poly(amide-hidrazide) (PAH) casting solutions result in a higher permeability without lowering selectivity [5]. Besides inorganic additives it is also common to use organic additives such as glycerol, polyethylene glycol (PEG) or polyvinylpyrrolidone

Abbreviations: AFM, atomic force microscopy; ATR–FTIR, attenuated total reflectance Fourier transform infra-red spectroscopy; CA, cellulose acetate; CTA, cellulose triacetate; DI water, Deionized water; DMA, dynamic mechanical analysis; DMF, N,N-Dimethylformamide; DSC, dynamic scanning calorimetry; EE, ethylether; EtOH, ethanol; EVAL, poly(ethylene-co-vinyl alcohol); HPLC, high pressure liquid chromatography; IPA, Isopropanol; MA, maleic acid; MAE, Mean Absolute Error; MAPE, Mean Absolute Percentage Error; MeOH, methanol; MIR, middle infrared; MSA, methane sulphonic acid; MSE, Mean Square Error; MW, molecular weight; MWCO, molecular weight cut-off; NF, nanofiltration; N-NMP, N-Methyl-2-pyrrolidone; OSN, organic solvent nanofiltration; PA, polyamide; PAH, poly(amide-hidrazide); PAH, poly(amide hydrazide; PEEK, poly(ether ether ketone); PEG, polyethylene glycol; PI, polyimide; PI, polyimide; PS, polystyrene; PSf, polysulphone; PVP, polyvinylpyrrolidone; RMSE, Root Mean Square Error; SA, sulphuric acid; SEM, scanning electron microscopy; TGA, thermal gravimetric analysis; TGS, triglycine sulphate; THF, tetrahydrofuran; UF, ultrafiltration; UV/Vis, ultraviolet/visible detector

* Corresponding author.
E-mail address: a.livingston@imperial.ac.uk (A. Livingston).

http://dx.doi.org/10.1016/j.memsci.2015.07.012

(PVP); for example, adding maleic acid (MA) to cellulose triacetate (CTA) increases the porosity and permeability [5,8].

The choice of the non-solvent (coagulation bath) affects the membrane morphology as well. The higher the rate of exchange between solvent and non-solvent the higher the porosity of the membrane; this is the case, for example, of the N-Methyl-2-pyrrolidone (N-NMP) /water (solvent/non-solvent) pair for polysulfone (PSf) membranes. It is also common to use additives like alcohols or DMF to vary the exchange rate of solvent/non-solvent. Another factor to take into account in the coagulation bath is the temperature. In general, an increase in the temperature of the coagulation bath leads to a higher exchange rate and consequently to a more porous structure [9].

In the post-casting treatment several factors such as temperature and time of evaporation, relative humidity of the air and air velocity (if a convective flow is applied) can affect the membrane performance. In terms of evaporation time there seems to be two contradictory effects. For membranes prepared from PA (polyamide), PAH (poly(amide hydrazide) and CA (cellulose acetate) the flux decreases and the rejection increases with increasing evaporation time. However, Soroko et al. [10] and See-Toh et al. [7] have concluded that increasing evaporation time reduces the flux but has no effect on rejection for polyimide (PI) membranes. In terms of temperature of evaporation, Young et al. [11] found that for poly(ethylene-co-vinyl alcohol) (EVAL)-although not used for OSN – a membrane structure with a particulate morphology was obtained at low temperatures after all the casting solution evaporated, while the rise in the evaporation temperature changed EVAL membrane structure from a particulate to a dense morphology. In addition, for PAH it was observed that with increasing temperature lower fluxes and higher rejections were obtained reaching a plateau at 100 °C; above this temperature inverse behaviour occurred in terms of solute rejection (probably due to polymer degradation) [9,12].

In order to stabilise and improve membrane performance there are several post-treatments that can be used such as annealing the membrane in water or under dry conditions, exposure to concentrated mineral acids, plasma treatment, drying with the solvent exchange technique and treatment with conditioning agents [5,13–16].

For most membranes prepared by wet phase inversion it is common for membranes to be stored under wet conditions because the structure of the membrane changes ("collapses") when the membrane is subjected to a drying process. In the case of ultrafiltration membranes (and nanofiltration as well) drying almost without exceptions induces irreversible loss of solvent permeance which is thought to be related to the collapse of the nodular structure [14]. In fact, using a multiple solvent exchange procedure can minimise the risk of nodule collapse upon drying. In this procedure, the residual non-solvent present in the membrane after immersion is replaced by a first solvent, which is miscible with the non-solvent; this solvent is then replaced by a more volatile solvent, which can be removed easily by evaporation to obtain a dry membrane [17–19]. One way to describe this nodular collapse is by using the theory introduced by Brown [20] for polymer latex particles during film formation. Beerlage [14] used this theory for PI ultrafiltration membranes and related the capillary forces (F_c) with the resistance of the matrix to deformation (F_r) developed by Brown. F_c is given by Eq. (1) where γ (N m^{-2}) is the surface tension of the gas/liquid interface inside the pores, r_p (m) is the pore radius, θ (deg) is the contact angle between the liquid and the membrane material and A (m^2) is the pore cross sectional area. F_r is given by Eq. (2) where E (N m^{-2}) is the tensile modulus of the polymer material and is a measure of the pore wall elasticity. According to this approach if $F_c > F_r$ then collapse of the nodular structure will occur (Eq. (3)).

$$F_c = \frac{2\gamma}{r_p}\cdot\cos\theta\cdot A \tag{1}$$

$$F_r = 0.37E\cdot\mathrm{A} \tag{2}$$

Thus for any given pore size the pore will collapse if

$$\frac{2\gamma\cdot\cos\theta}{r_p} > 0.37\times E \tag{3}$$

Based on the decrease of surface tension (for example via solvent exchange) it is possible to maintain the pore structure of a membrane (i.e. to minimise the capillary force) if the strength of the matrix is high enough [14,18–21].

In a previous work we introduced the excellent stability and performance of native PEEK nanofiltration membranes prepared in our laboratory [22]. This research work communicates a detailed investigation of the production of non-sulphonated nanofiltration PEEK membrane with a MWCO around 350–500 g mol^{-1}, resistant to polar aprotic solvents (such as DMF), high temperature, acids and bases [1]. Different factors affecting membrane separation performance are studied including polymer concentration in the dope solution and membrane post-treatment procedures. It has been shown that the post-manufacturing membrane drying step is of vital importance for the membrane nanofiltration performance.

2. Methods

2.1. Materials

2,4-Diphenyl-4-methyl-1-pentene (α-methyl styrene dimer) and methane sulphonic acid (MSA) were obtained from Sigma-Aldrich. N,N-Dimethylformamide (DMF), tetrahydrofuran (THF), propanone (acetone), 2-propanol (IPA), methanol (MeOH), ethanol (EtOH), n-hexane, heptane, acetonitrile and sulphuric acid (SA) 95 vol% were obtained from VWR UK. VESTAKEEP® 2000P and 4000P were kindly obtained from Evonik Industries; VICTREX® 150P and 450P were kindly donated by VICTREX®. The styrene oligomers standards with a molecular weight distribution of 580 (PS580) and 1300 (PS1300) were obtained from Agilent Technologies Deutschland GmbH, Germany. All reagents were used as received without any further purification.

2.2. Membrane preparation

PEEK powder VESTAKEEP® 4000P was dissolved at a concentration of 8 wt%, 10 wt% and 12 wt% in a mixture of 3:1 wt% methanesulfonic acid (MSA) and sulphuric acid (SA) by mechanical stirring (IKA RW 20 digital) at 20 °C until complete homogenisation of polymer solution. Prior to casting the polymer solution was left 72–96 h at 20 °C until complete removal of air bubbles. The membranes were cast using a bench top laboratory casting machine (Elcometer 4340 Automatic Film Applicator) with a blade film applicator (Elcometer 3700) set at 250 μm thickness. The polymer dope solution obtained was poured into the blade and cast on a non-woven polypropylene support (Novatex 2471, Freudenberg Filtration Technologies Germany) with a transverse speed of 0.5 cm s^{-1}. Following this, the membranes were immersed in a deionised (DI) water precipitation bath at 20 °C; the water in the bath was changed several times until pH was 6–7. For the membranes produced with a 12 wt% polymer concentration a solvent exchange from water to IPA, MeOH, n-hexane, EtOH, acetone, THF, heptane or acetonitrile was performed. Finally, the membranes were left to dry at either 20 °C, 40 °C, 80 °C, 120 °C or

Fig. 1. Schematic representation of the steps involved in the PEEK membrane preparation.

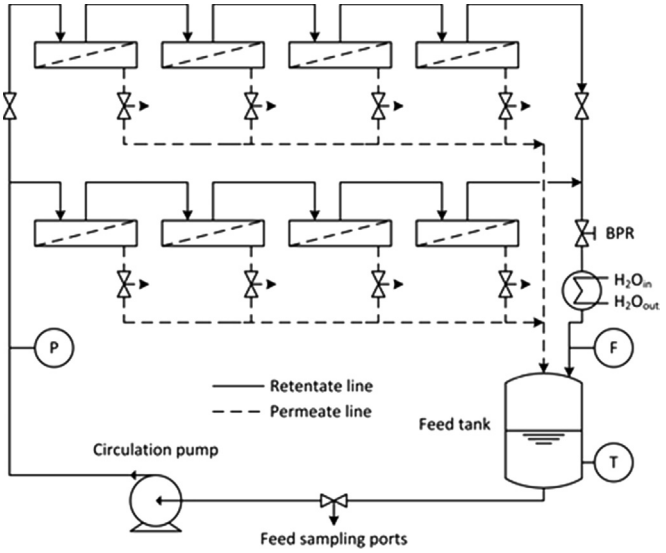

Fig. 2. Schematic representation of the 8 cells cross-flow rig used in this study. P – pressure gauge; T – thermocouple; F – flow metre; BPR – back pressure regulator.

140 °C[1] (reported as the glass transition temperature for PEEK) [12,23]. Membrane preparation steps are represented in Fig. 1. The viscosity of the dope solution was measured immediately after casting using a rotary viscometer (LV-2020 Rotary Viscometer Cannon instruments, S16 spindle) and all values were recorded at 1 rpm spindle speed and 20 °C.

All the membrane formation steps were performed in an air conditioned room set at 20 °C and with a relative humidity (RH) in the range of 30–40%.

2.3. Membrane characterisation

2.3.1. Thermal gravimetric analysis (TGA)

TGA measurements of PEEK samples were performed using a TGA Q500 (TA Instruments) and 100 μL platinum pans. The measurements were done under nitrogen and oxygen atmosphere and a gas flow of 40 mL min^{-1} for nitrogen and 60 mL min^{-1} for air. The heating rates varied between 10 K min^{-1} and 40 K min^{-1} and each sample was maintained at the target temperatures – 20 °C, 40 °C, 80 °C, 100 °C and 120 ° – for 400 min (isothermal step).

2.3.2 Dynamic mechanical analysis (DMA)

Rectangular specimens of water "wet" membranes having a size of 35 mm × 6 mm × 0.2 mm ($L \times W \times H$) were used for the dynamic mechanical experiments. Dynamic mechanical thermal analyser (Tritec 2000DMA, TA Instruments) was used for the evaluation of the dynamic modulus (stiffness) and mechanical damping (tan δ). Membrane properties were measured over the temperature range from 25 to 120 °C at a heating rate of 2 K min^{-1}. The tests were carried out at 1 Hz with a displacement of 0.05 mm.

[1] The drying temperature of 140 °C was only used for membranes dried from water.

2.3.3 Dynamic scanning calorimetry (DSC)

Changes in the degree of crystallinity of the samples during drying were observed by differential scanning calorimetry (DSC) (DSC Q200, TA Instruments). Samples were heated from 20 to 400 °C at a constant ramp rate of 10 °C min^{-1} in DSC aluminium pans (heating cycle 1). After cooling down at a rate of 10 °C min^{-1} to 20 °C the samples were heated using the same method as the one used in heating cycle 1 (heating cycle 2). A sharp peak at about 330–340 °C is characteristic of PEEK crystal melting. The area under the melting curve was used to calculate the heat required for the melting process. The heat of melting for a 100% crystalline PEEK sample is 130 J g^{-1}[23]. Thus, the ratio of the two heats of melting was calculated to obtain the degree of crystallinity of the sample.

2.3.4 Scanning electron microscopy (SEM)

For cross-section imaging a membrane sample was broken in liquid nitrogen and pasted vertically onto SEM stubs covered with carbon tape. For surface imaging a membrane sample was cut and pasted horizontally onto SEM stubs covered with carbon tape. The samples were then coated with a chromium-layer in an Emitech K575X peltier under an argon atmosphere to reduce sample charging under the electron beam. SEM pictures of the surface and cross section of membrane samples were recorded using a Scanning electron microscope of low resolution (JEOL 6400) at 20 KV and under dry conditions at room temperature.

2.3.5 Membrane performance and analysis

ZIn order to test the membranes a rig with 8 membrane cross-flow cells was used (effective membrane area = 14 cm^2 at each cell, see Fig. 2). PEEK membranes were initially conditioned by passing pure solvent through at 30 °C and 30 bar (for 1 h). Polystyrene standard solution was then poured into the feed reservoir and the system was pressurised again up to 30 bar and the temperature set at 30 °C.

The polystyrene standard solution was prepared by dissolving 2,4-Diphenyl-4-methyl-1-pentene (dimer, M_W = 236 g mol^{-1}) and Polystyrene Standards with a M_W ranging from 295 to 1995 g mol^{-1} (homologous series of styrene oligomers (PS)) in DMF or THF at a concentration of 1 g L^{-1} each M_W. Permeate and retentate samples were collected at different time intervals for rejection determination. Concentrations of PS in permeate and retentate samples were analysed using an Agilent HPLC system with a UV/Vis detector set at a wavelength of 264 nm. Separation was accomplished using an ACE 5-C18-300 column (Advanced Chromatography Technologies, ACT, UK). A mobile phase comprising 35 vol% analytical grade water and 65 vol% tetrahydrofuran (THF) both containing 0.1 vol % trifluoroacetic acid was used [24].

The flux (J) and permeance (L_P) were determined using Eqs. (4) and (5) and the rejection (R_i) of PS was evaluated applying Eq. (6). The corresponding MWCO curves were obtained from a plot of the rejection of PS versus their molecular weight. To eliminate the effect of compaction typically observed over the first 2–5 h of experiment, for membrane performance comparison purposes only the steady state flux (after 24 h) was considered (steady state flux was considered achieved when two flux (permeance) measurements within a 1 h interval showed the same value within ± 0.02 L m^{-2} h^{-1} bar^{-1}).

$$J\left[\mathrm{L\,h^{-1}\,m^{-2}}\right] = \frac{\text{Flow rate}\left[\mathrm{L\,h^{-1}}\right]}{\text{Membrane area}\left[\mathrm{m^2}\right]} \quad (4)$$

$$L_p\left[\mathrm{Lh^{-1}m^{-2}bar^{-1}}\right] = \frac{J\left[Lh^{-1}\mathrm{m^{-2}}\right]}{\triangle p\ [\mathrm{bar}]} \quad (5)$$

$$R_i\ [\%] = \left(1 - \frac{C_{P,i}}{C_{F,i}}\right) \times 100 \quad (6)$$

2.4 Experimental design

The methodology used in this study was based on the comparison of PEEK membranes dried at 120 °C and produced either with different polymer concentrations (8 wt%, 10 wt% and 12 wt%) or dried from different solvents (solvent exchange) in terms of performance (permeance and rejection). For each of the different membranes four replications were performed in order to have a statistically robust sample. All the results were analysed using *F*-test. For the permeance data the *F*-test was used for permeance values obtained after 24 h. For rejection data the *F*-test was applied to each individual polystyrene (PS), i.e. for each solute size (different MW) the four different membranes were compared with each other. Statistical significance was considered at $p < 0.05$. Data are presented as means ± standard deviation of the mean (SDM).

3. Results and discussion

3.1 Control of pore collapsing for tuning MWCO

3.1.1 The effect of polymer concentration and drying temperature

As reported previously, the nanofiltration properties of PEEK membranes are correlated to the drying of the membranes [21]. Nevertheless, the permeance values reported were relatively low. In order to improve the permeance – without compromising the MWCO – a study on polymer concentration (8–12 wt%) and drying temperatures (20 °C, 40 °C, 80 °C and 120 °C) was performed in order to determine their influence on membrane performance (Table 1).

As expected, the membranes with lower polymer concentration (8 wt%) presented higher permeance values, in the range of 1.25–2.30 L h^{-1} m^{-2} bar^{-1}, and a MWCO in the range of 795–1295 g mol^{-1} (Fig. 3). Interestingly, the membranes dried at 20 °C and 120 °C were the tightest ones and with lower permeance whereas the ones dried at 40 °C and 80 °C presented a higher MWCO and higher permeance, i.e., there was no trend as a function of the temperature. Both higher polymer concentrations – 10 wt% and 12 wt% – presented lower permeances and lower MWCO (tighter membranes). The permeance of the membranes prepared with 10 wt% of polymer was in the range of 0.42–0.52 L.h^{-1} m^{-2} bar^{-1} and the MWCO was in the range of 395 –495 g mol^{-1}. As for the 12 wt% membranes, the permeance was in the range of 0.18–0.40 L h^{-1} m^{-2} bar^{-1} and the MWCO was in the range of 295–395 g mol^{-1}. It can be seen from the different membranes dried at 120 °C (Fig. 4) that the polymer concentration had a greater influence on membrane performance than drying temperature (Fig. 3). The difference was more noticeable between the 8 wt% and the 10 wt% than between the 10 wt% and the 12 wt%. The difference in performance for different polymer concentrations could be explained by the viscosity of the dope solution, because the 8 wt% polymer dope solution had 3.30 times and 7.51 times lower viscosity than the 10 wt% polymer dope and 12 wt% polymer dope respectively. In contrast, the difference in viscosity between 10 wt% polymer dope solution and 12 wt% polymer dope solution was only 2.28 times. The viscosity of the dope solution (Table 1) could explain the results obtained because higher casting solution viscosities slow down non-solvent in-diffusion and demixing is delayed, resulting in membranes with thicker and denser skin-layers and sublayers with lower porosities. From the SEM images (Fig. 4 bottom) it was found that membranes PM-B 8 wt% 120 °C had a thinner active layer of approximately 2.0 μm whereas for membranes with higher polymer concentration the active layer had a thickness of approximately 2.9 μm.

There is no sharp border line between MWCO of the different membrane separation processes, however in general nanofiltration is considered to cover separations of molecules within the 200–2000 Da range [3]. As such all PEEK membranes reported in this study are nanofiltration membranes. However currently the organic solvent nanofiltration membranes market suffers a lack of "tight" membranes with MWCO at the lowest range of nanofiltration, ~200 Da, that can be used for example for solvent recovery. To the best of our knowledge there is only one OSN membrane on the market claiming MWCO of 150 Da – Duramem150 manufactured by Evonik Industries. That is why we have chosen to investigate further the tightest membrane from the PEEK series in an attempt to manipulate its MWCO and eventually make it tighter. Given the fact that the membranes with a polymer concentration of 12 wt% presented the lowest MWCO, all

Table 1
Summary of PEEK membranes PM-B prepared from dopes with different polymer concentrations (8 wt%, 10 wt% and 12 wt%) and dried from water at different temperatures. The viscosity (Pa s) of the membrane dope solution as well as the spindle speed (rpm) used are presented in this table. These membranes were used to test the influence of polymer concentration and drying temperature on permeance and rejection.

Membrane code	Polymer concentration (wt%)	Viscosity (Pa s)	Spindle speed (rpm)	Drying temperature (°C)
PM-B 8 wt% 20 °C	8	7.72 ± 0.04	10	20
PM-B 8 wt% 40 °C				40
PM-B 8 wt% 80 °C				80
PM-B 8 wt% 120 °C				120
PM-B 10 wt% 20 °C	10	25.46 ± 1.86	3	20
PM-B 10 wt% 40 °C				40
PM-B 10 wt% 80 °C				80
PM-B 10 wt% 120 °C				120
PM-B 12 wt% 20 °C	12	58.03 ± 1.58	1	20
PM-B 12 wt% 40 °C				40
PM-B 12 wt% 80 °C				80
PM-B 12 wt% 120 °C				120

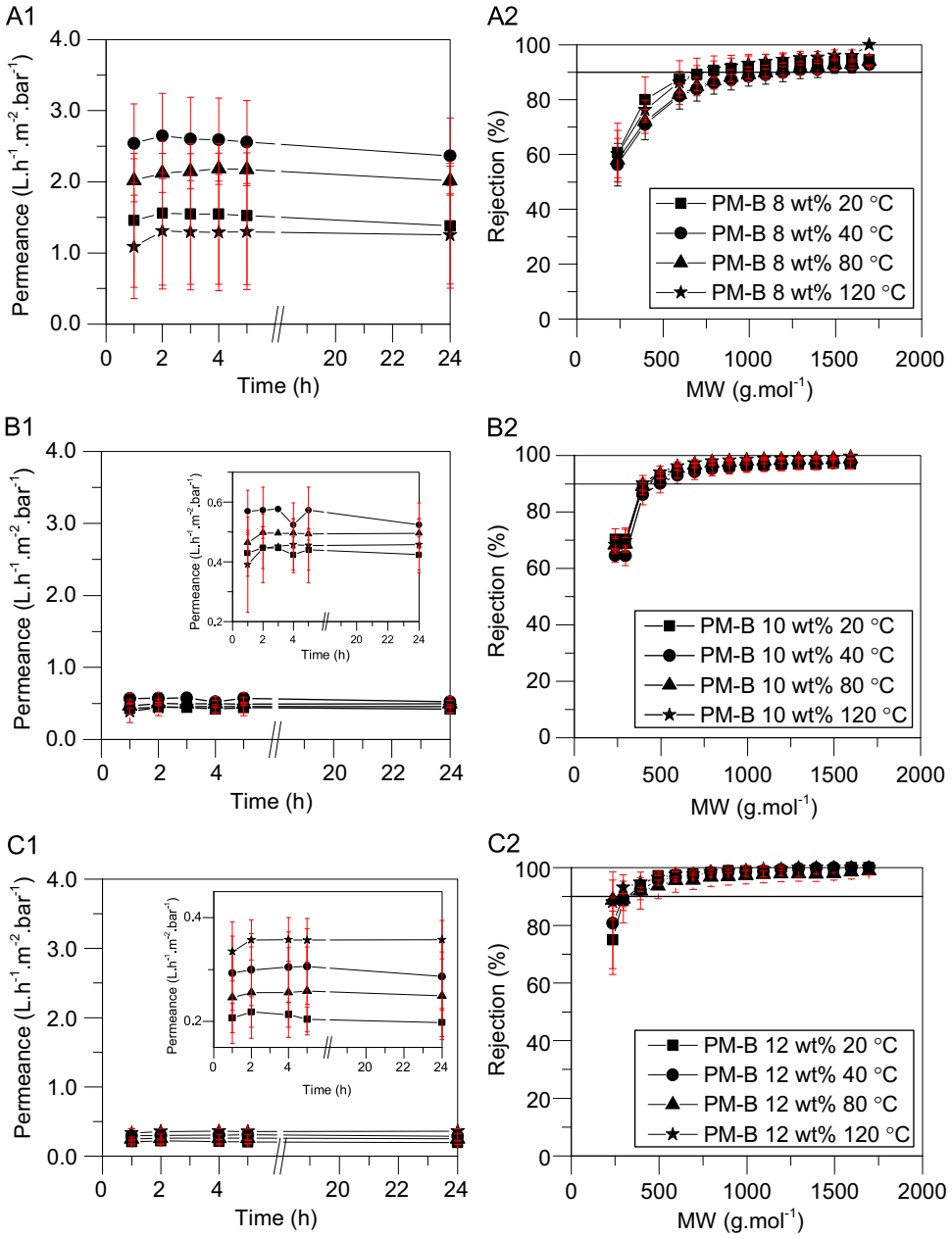

Fig. 3. A1, B1 and C1: Permeance values (L h^{-1} m^{-2} bar^{-1}) over a period of 24 h for the different membranes under study. A2, B2 and C2: Rejection values of the different PEEK membranes under study as a function of the molecular weight (M_W, g mol^{-1}) of different polystyrenes after 24 h. All the membranes presented were dried from water at different temperatures (20 °C, 40 °C, 80 °C and 120 °C) prior to their insertion in the cross-flow cells. The membranes were filtered with a solution of THF and PS (1 g L^{-1}). The flow-rate, temperature and pressure were set at 100 L h^{-1}, 30 °C and 30 bar, respectively. The red bars represent the standard deviation of the mean. (For interpretation of the references to color in this figure legend, the reader is referred to the web version of this article.)

subsequent studies in this research work were performed using this polymer concentration.

3.1.2 The effect of drying solvent

As already mentioned in Section 2 of the manuscript, according to the literature [14,20], the final membrane pore size is greatly influenced by the surface tension of the solvent filling membrane pores prior to drying. To investigate this effect on the PEEK membranes a solvent exchange from water to IPA, MeOH, EtOH, n-hexane, acetone or THF was performed after the phase inversion process in order to change the surface tension and possibly achieve different extents of collapsing in the polymer nodular structure. Water has a surface tension of 72.8 mN m^{-1} while the remaining solvents have similar (and much lower) values of surface tension in the range of 18.4–26.4 mN.m^{-1} (Table 2).

The contact angle water/PEEK was measured to be 60°. We were unable to measure contact angles for the other solvents, since the droplet spread instantaneously, thus these contact angles were assumed as 0°. Therefore, and according to the theory presented by Brown (Eq. (3)) [20], membranes immersed in IPA, MeOH, EtOH should give similar MWCO because of the similarity in surface tension; n-hexane should present higher MWCO (looser membranes) because it has the lowest surface tension and acetone and THF should give tighter membranes (excluding the ones dried from water). According to this method F_c should be higher for water at any given pore radius and therefore, pore collapse in water is expected to occur at a much higher extent. As a result, membranes dried from all the other solvents should be looser than membranes dried from water with the following order (from lower MWCO to higher MWCO membrane):

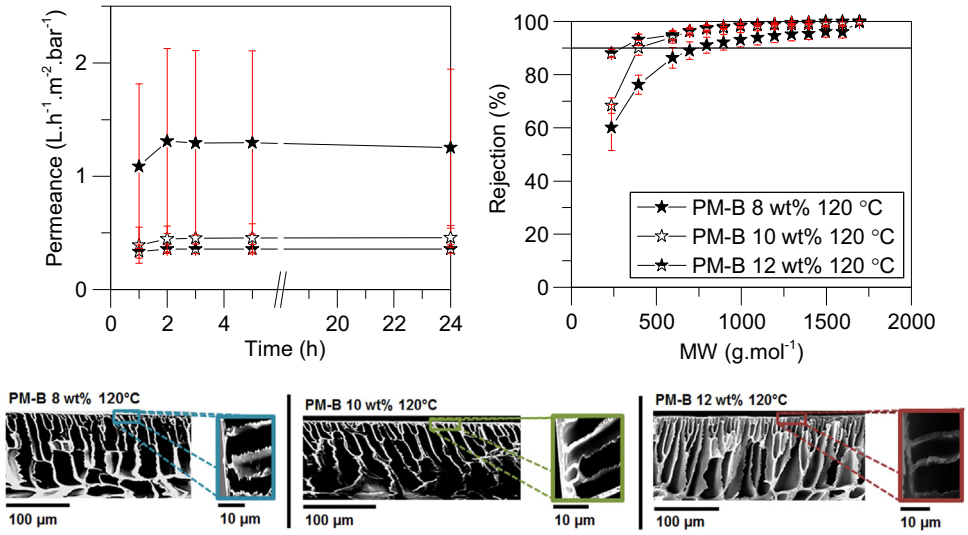

Fig. 4. Top left: Permeance values (L h^{-1} m^{-2} bar^{-1}) over a period of 24 h for the different membranes under study. Top right: Rejection values of the different PEEK membranes under study as a function of the molecular weight (M_W, g mol^{-1}) of different polystyrenes after 24 h. All the membranes presented were dried from water at 120 °C prior to their insertion in the cross-flow cells. The membranes were filtered with a solution of THF and PS (1 g L^{-1}). The flow-rate, temperature and pressure were set at 100 L h^{-1}, 30 °C and 30 bar, respectively. The red bars represent the standard deviation of the mean. The membranes dried from water at 120 °C are significantly different ($p \leq 0.05$, *F*-test). Bottom: Cross-section SEM images (magnification 300 ×) of the different membranes under study: PM-B 8 wt% 120 °C, PM-B 10 wt% 120 °C and PM-B 12 wt% 120 °C. (For interpretation of the references to color in this figure legend, the reader is referred to the web version of this article.)

Table 2
Summary of PEEK membranes PM-B 12 wt% prepared from different dopes and with different post-treatments. These membranes were used to test the influence of solvent exchange and drying temperature on permeance and rejection. In addition, properties of the solvents used for the solvent exchange: surface tension (mN m^{-1}), M_W (g mol^{-1}), boiling point (°C), vapour pressure (kPa) and molar volume (cm^3 mol^{-1}). All properties listed were obtained from [25] at 20 °C and 1 bar.

Membrane code	Drying solvent	Drying temperature (°C)	**Solvent properties**			
			Surface tension (mN m^{-1})	Boiling point (°C)	Vapour pressure (kPa)	Molar volume (cm^3 mol^{-1})
PM-B1.1	Water	20	72.8	100	2.33	18.0
PM-B1.2	Water	40				
PM-B1.3	Water	80				
PM-B1.4	Water	120				
PM-B2.1	MeOH	20	22.6	64	16.93	40.6
PM-B2.2	MeOH	40				
PM-B2.3	MeOH	80				
PM-B2.4	MeOH	120				
PM-B3.1	EtOH	20	22.3	78	5.95	58.6
PM-B3.2	EtOH	40				
PM-B3.3	EtOH	80				
PM-B3.4	EtOH	120				
PM-B4.1	IPA	20	21.7	82	4.10	76.9
PM-B4.2	IPA	40				
PM-B4.3	IPA	80				
PM-B4.4	IPA	120				
PM-B5.1	Acetone	20	23.3	56	30.80	73.8
PM-B5.2	Acetone	40				
PM-B5.3	Acetone	80				
PM-B5.4	Acetone	120				
PM-B6.1	THF	20	26.4	66	21.60	81.9
PM-B6.2	THF	40				
PM-B6.3	THF	80				
PM-B6.4	THF	120				
PM-B7.1	n-hexane	20	18.4	69	20.17	131.4
PM-B7.2	n-hexane	40				
PM-B7.3	n-hexane	80				
PM-B7.4	n-hexane	120				

water < THF < acetone < MeOH < EtOH < IPA < n-hexane. Together with the solvent type the effect of drying temperature on the permeance and on the MWCO was also studied. The membranes produced are presented in Table 2.

As mentioned before in Section 3.1.1, the permeance for all membranes dried from water at different temperatures had permeance values in the range of 0.20–0.36 L h^{-1} m^{-2} bar^{-1}. The membranes dried from water at 120 °C had almost double the permeance of membranes dried at 20 °C. This fact could be attributed to residual water that may have been retained in the smallest pores (thus obstructing solvent permeance), whilst above 100 °C (boiling point of water at 1 bar) all residual water may have been completely removed (hence higher permeance). Another interesting result was to determine the effect of temperature on the degree of crystallinity of the membranes dried from water (Fig. 13 Appendix). It can been seen that from PM-B1.1 (dried at 20 °C) to PM-B1.4 (dried at 120 °C) there were no changes in the membrane crystallinity. A membrane dried at 140 °C was also prepared. It showed THF permeance of 0.04 L h^{-1} m^{-2} bar^{-1} but no rejection in the NF range (data not shown), possibly due to defects originating from the partial melting of the backing material, and was not further investigated. Thus all further drying experiments were limited to 120 °C.

As for membranes dried from the alcohols, it can be observed that for MeOH (Fig. 5A1 and A2) the permeance values varied more with the temperature ranging from 1.07 L h^{-1} m^{-2} bar^{-1} (PM-B2.4) to 2.3 L h^{-1} m^{-2} bar^{-1} (PM-B2.3). From the rejection data (Fig. 5A2) it can be observed that the drying temperature has a greater effect on the MWCO, i.e, the higher the drying temperature the tighter the membrane. For the temperatures of 40 °C and 80 °C the rejection values were in fact quite similar, although the variability of the membranes PM-B2.2 and PM-B2.3 makes it difficult to confirm this result. The loosest membrane, PM-B2.1, has a MWCO beyond the NF range. Membranes PM-B2.2 and PM-B2.3

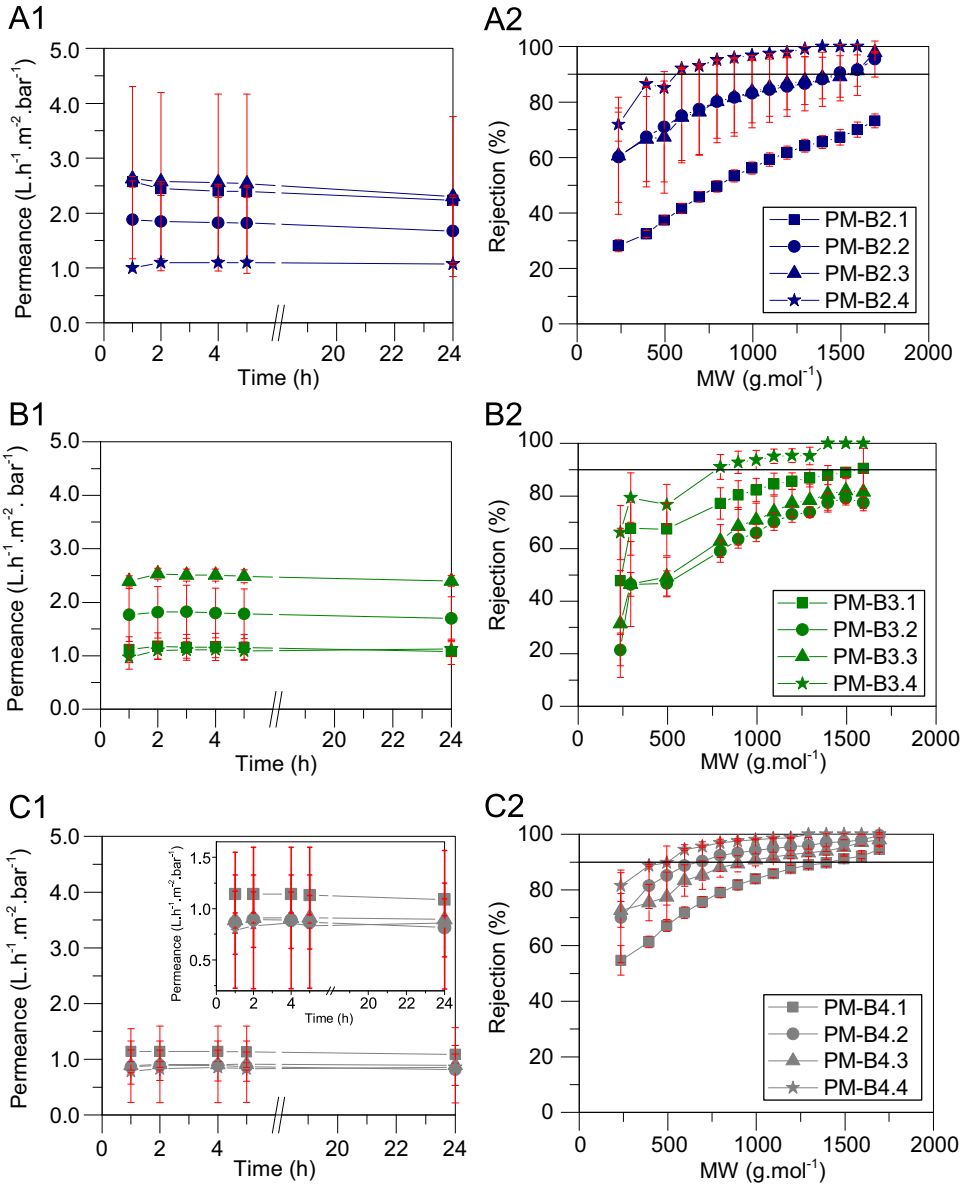

Fig. 5. A1, B1 and C1: Permeance values (L h^{-1} m^{-2} bar^{-1}) over a period of 24 h for the different membranes under study. A2, B2 and C2: Rejection values of the different PEEK membranes under study as a function of the molecular weight (M_W, g mol^{-1}) of different polystyrenes after 24 h. Membranes PM-B2.*x*, PM-B3.*x* and PM-B4.*x* (*x*=1, 2, 3 and 4) were dried from MeOH, EtOH and IPA respectively at different temperatures (20 °C, 40 °C, 80 °C and 120 °C) prior to their insertion in the cross-flow cells. The membranes were filtered with a solution of THF and PS (1 g L^{-1}). The flow-rate, temperature and pressure were set at 100 L h^{-1}, 30 °C and 30 bar, respectively. The red bars represent the standard deviation of the mean. (For interpretation of the references to color in this figure legend, the reader is referred to the web version of this article.)

presented a MWCO of around 1300 g mol^{-1}, but the standard deviation was not narrow enough to validate the result. The tightest membrane, PM-B2.4, had a MWCO around 600 g mol^{-1}.

For the membranes dried from EtOH (Fig. 5B1 and B2) the permeance varied from 1.07 L h^{-1} m^{-2} bar^{-1} (PM-B3.1) to 2.1 L h^{-1} m^{-2} bar^{-1} (PM-B3.3). From the rejection data (Fig. 5B2) one can observe that for the temperatures of 40 °C and 80 °C the rejection values were quite similar and both had a MWCO beyond the NF range; membrane PM-B3.1 presented a MWCO of around 1595 g mol^{-1}; and the tightest membrane, PM-B3.4, had a MWCO around 795 g mol^{-1}.

For the membranes dried from IPA (Fig. 5C1 and C2) the permeance was on average 3.5 times higher than the membranes dried from water. In fact, the values of permeance ranged from 0.81 L h^{-1} m^{-2} bar^{-1} (PM-B4.2, dried at 40 °C) to 1.36 L h^{-1} m^{-2} bar^{-1} (PM-B4.4 dried at 20 °C). Analysing the rejection data it can be seen that the higher the drying temperature, the tighter the membrane, with the exception of PM-B4.2 (dried at 40 °C). For temperatures of 40 °C and 80 °C the rejection values were quite similar, although slightly higher for PM-B4.2 (as mentioned above). The membrane with the lowest permeance (PM-B4.4) presented the lowest MWCO and its value was around 500 g mol^{-1}. For membrane PM-B4.1 (membrane with a high permeance) the MWCO was in the upper range of NF with a value around 1400 g mol^{-1}.

In the case of alcohols, we speculate that the boiling points of each of the alcohols are lower than the boiling point of water (Table 2) which allows for more solvent to be removed from the membrane pores at a faster rate; therefore, the drying temperature had more pronounced effect on the properties of the membrane when compared with water.

Fig. 6D and E shows that membranes dried from acetone and

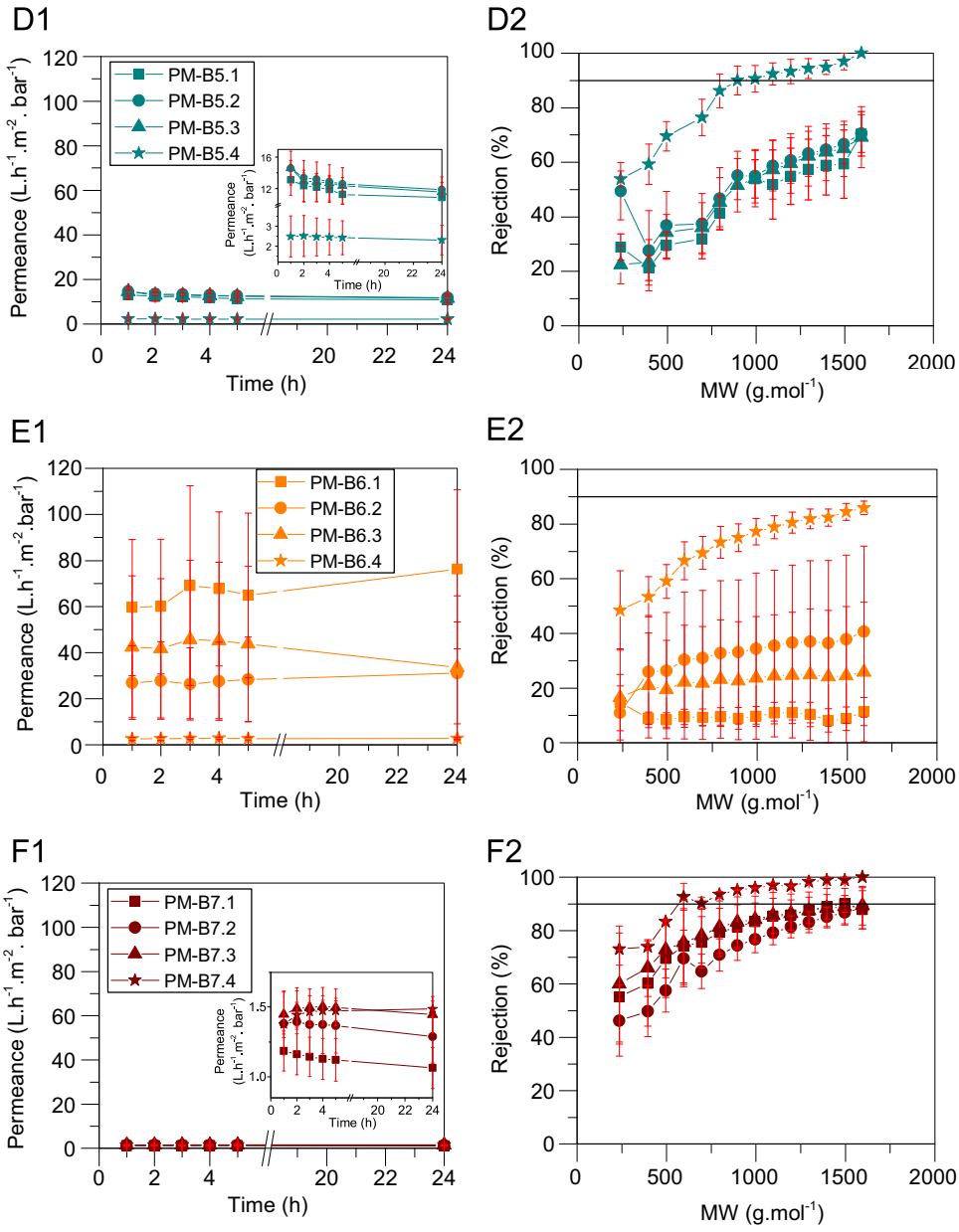

Fig. 6. D1, E1 and F1: Permeance values (L h^{-1} m^{-2} bar^{-1}) over a period of 24 h for the different membranes under study. D2, E2 and F2: Rejection values of the different PEEK membranes under study as a function of the molecular weight (M_W, g mol^{-1}) of different polystyrenes after 24 h. Membranes PM-B5.*x*, PM-B6.*x* and PM-B7.*x* (x=1, 2, 3 and 4) were dried from acetone, THF and n-hexane respectively at different temperatures (20 °C, 40 °C, 80 °C and 120 °C) prior to their insertion in the cross-flow cells. The membranes were filtered with a solution of THF and PS (1 g L^{-1}). The flow-rate, temperature and pressure were set at 100 L h^{-1}, 30 °C and 30 bar, respectively. The red bars represent the standard deviation of the mean. (For interpretation of the references to color in this figure legend, the reader is referred to the web version of this article.)

THF were affected to a greater extent by the temperature. For both solvents (acetone and THF), the membranes had similar performances at 20 °C to 80 °C, but a substantial difference arose when dried at 120 °C (Fig. 6D2 and E2). In the case of acetone, the membranes dried at 120 °C had a permeance of 2.15 L h^{-1} m^{-2} bar^{-1} which was on average 4.5 times lower than for any other drying temperature considered; the MWCO was 895 g mol^{-1} while for the other drying temperatures the membranes produced were not in the NF range. For the membranes dried from THF over the temperature range of 20–80 °C the standard deviations made it difficult to assess within a confidence interval either permeance and rejection. Nevertheless, for a temperature of 120 °C the membranes presented a permeance of 2.72 L h^{-1} m^{-2} bar^{-1} which was on average 28 times lower than PMB-6.1 and 12 times lower than PMB-6.2 and PMB-6.3. This membrane did not present a MWCO in the NF range, but nevertheless from Fig. 6E2 one can observe that a shift occurred in terms of rejection when comparing PM-B6.4 with the other membranes, presumably due to tightening of the membrane matrix by increasing drying temperature.

For membranes dried from n-hexane the temperature effect was not that pronounced but nevertheless the membranes dried at 120 °C were tighter (MWCO = 595 g mol^{-1}) than the ones dried at other temperatures which had similar performances (MWCO around 1400 g mol^{-1}). The permeance ranged from 1.06 L h^{-1} m^{-2} bar^{-1} to 1.49 L h^{-1} m^{-2}.bar^{-1}. It is also important to point out that membranes dried from n-hexane had two solvent exchanges from water to IPA and then to n-hexane. In this particular case water and IPA could still be present in the smaller pores and the drying solvent might not have been pure n-hexane but a mixture of the three (although IPA and water should be present in very small amounts).

In order to investigate whether the solvent was completely removed after 24 h at 20 °C and 120 °C membranes PM-B1.4, PM-B3.4 and PM-B6.4 were further dried using a vacuum oven at 120 °C. From Fig. 7 one can observe that the membranes PM-B1.4 and PM-B3.4 did not change in terms of rejection performance once vacuum drying was applied. Only a slight increase of the permeance was observed, suggesting some residual solvent may still be present in the smallest pores, but this does not significantly affect the separation properties. However, for membrane PM-B6.4 there was as a decrease in permeance of about two times and the membrane was tighter after vacuum oven was applied (MWCO ~ 1395 g mol^{-1}). This shows that for looser membranes there might be rearrangement of the polymeric structure and further nodule collapse from vacuum treatment. Nevertheless, there seems to be a physical limit in the collapse; the membrane did not collapse completely to, for example, the same degree as water dried membrane.

The influence of drying time and cool-down rate were also evaluated (Table 3). Experimental data showed that regardless of the drying time, 0.5 h or 24 h, the membrane performance does not change (Fig. 8). This means that an air-drying treatment at 120 °C for 0.5 h was sufficient to provide the same performance when 24 h was applied which constitutes considerable energy savings from a process point of view. In terms of cooling-down rate, there was no difference between instantaneous cool-down (∞) or 40 °C h^{-1} cool-down rate, further indicating that the membrane reaches a "frozen" and stable state once it is heated at 120 °C.

Apparently the correlation proposed by Brown and adopted by Beerlage [14] and by Gevers et al. [26], can describe only to a limited extent the results obtained. This correlation accounts only for surface tension, but not for other solvent properties, which may be important during membrane drying, such as boiling point, vapour pressure, Hansen solubility parameter, viscosity and molar volume. Brown's correlation is also based on the assumption that a complete solvent exchange has taken place in all of the membrane pores. However this may not be the case if some residual water is retained into the smallest membrane pores, or some of the pores are filled with solvent mixtures with properties (specifically surface tension) different from the pure solvent.

Our findings are in agreement with literature studies. Matsuyama et al. [27] performed and extensive study on the effect of drying on the structure of microporous polyethylene membranes. They observed that polymer film contraction can be attributed to a combination of two physical phenomena: densification of the amorphous regions of the film and collapse of pores due to capillary forces (Fig. 9). They investigated 11 different solvents and concluded that membrane porosity is inversely proportional to the solvent surface tension and the boiling point of the solvent. These authors hypothesised that pore collapse involves rearrangement of the amorphous polymer molecules within the matrix phase. Since such a rearrangement requires time, it is hypothesized that the longer the capillary force is in effect, the greater the time for rearrangement of polymer chains in the matrix phase and the greater the extent of pore collapse. This rather logical hypothesis explains well our experimental results and the difference between the membranes dried from the different solvents. Having a lower boiling point and higher vapour pressure, acetone and THF

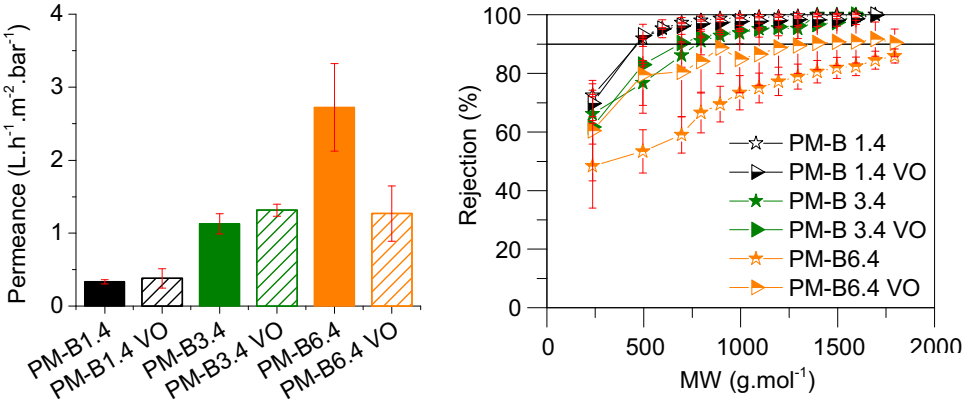

Fig. 7. Left: Permeance values (L h^{-1} m^{-2} bar^{-1}) at 24 h for the different membranes under study. Right: Rejection values of the different PEEK membranes under study as a function of the molecular weight (M_W, g mol^{-1}) of different polystyrenes after 24 h. All the membranes presented were at least dried from water, EtOH, acetone and THF at 120 °C and some were further dried in a vacuum oven (code VO) at 120 °C for 24 h prior to their insertion in the cross-flow cells. The membranes were filtered with a solution of THF and PS (1 g L^{-1}). The flow-rate, temperature and pressure were set at 100 L h^{-1}, 30 °C and 30 bar, respectively. The red bars represent the standard deviation of the mean. (For interpretation of the references to color in this figure legend, the reader is referred to the web version of this article.)

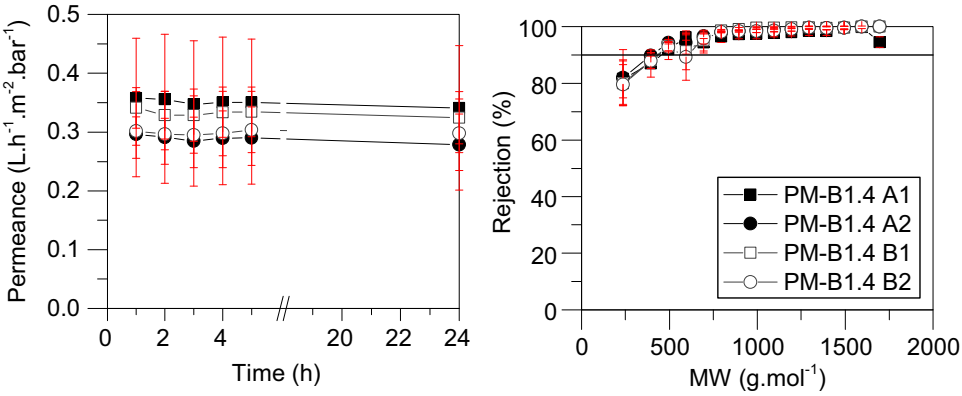

Fig. 8. Left: Permeance values (L h^{-1} m^{-2} bar^{-1}) over a period of 24 h for the different membranes under study. Right: Rejection values of the different PEEK membranes under study as a function of the molecular weight (M_W, g mol^{-1}) of different polystyrenes after 24 h. All the membranes presented were dried from water at 120 °C for 0.5 h (A) or for 24 h (B) and cool downed slowly (1) or fast (2) prior to their insertion in the cross-flow cells. The membranes were filtered with a solution of THF and PS (1 g L^{-1}). The flow-rate, temperature and pressure were set at 100 L.h^{-1}, 30 °C and 30 bar, respectively. The red bars represent the standard deviation of the mean. (For interpretation of the references to color in this figure legend, the reader is referred to the web version of this article.)

Table 3
Summary of PEEK membranes PM-B prepared from different dopes and with different post-treatments. These membranes were used to test the influence of drying time and cool-down rate on permeance and rejection.

Membrane code	Drying solvent	Drying temperature (°C)	Drying time (h)	Cool-down rate (°C h^{-1})
PM-B1.4A1	Water	120	0.5	40
PM-B1.4A2	Water	120	0.5	∞ (Instantaneous)
PM-B1.4B1	Water	120	24	40
PM-B1.4B2	Water	120	24	∞ (Instantaneous)

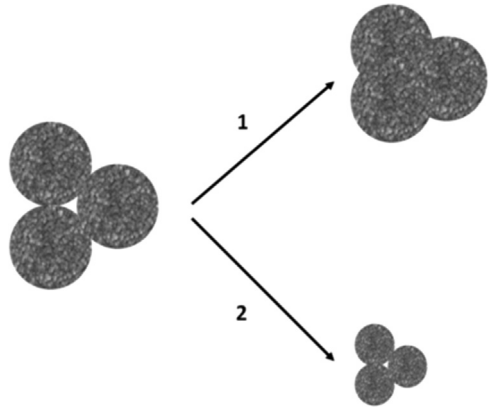

Fig. 9. Schematic representation of the two physical phenomena methods proposed by Matsuyama et al. [27]: 1 – collapse of pores due to capillary forces and 2 – densification of the amorphous regions of the film.

disappear much faster from the membrane pores, shortening the action time of capillary force applied and the degree of pore collapse. However it somewhat contradicts the general trend for decrease of the membrane MWCO with the increase of the drying temperature observed with all solvents. The latter effect may be attributed to a larger contribution of the second phenomenon – densification of the amorphous regions due to polymer chain relaxation. In any case it is clear that the change from ultrafiltration to nanofiltration in our PEEK membranes is due to a secondary rearrangement of the polymeric chains during the drying–heating–cooling post-manufacturing treatment.

Other studies also pointed out similar effects of the solvent boiling point [28] and the drying temperature [29] on the membrane permeance and MWCO. Interestingly a few studies [17,28,29] present a correlation between the polymer-drying solvent affinity (expressed in terms of the Hansen solubility parameter) and the dried membrane properties. For our case study the solubility parameter for PEEK at 20 °C is reported as 9.5 $(cal\ cm^{-3})^{0.5}$ vs. water – 25.5 $(cal\ cm^{-3})^{0.5}$, methanol – 14.5 $(cal\ cm^{-3})^{0.5}$, IPA – 11.5 $(cal\ cm^{-3})^{0.5}$, EtOH – 13.4 $(cal\ cm^{-3})^{0.5}$, n-hexane – 6.9 $(cal\ cm^{-3})^{0.5}$, acetone – 10 $(cal\ cm^{-3})^{0.5}$ and THF – 9.1 $(cal\ cm^{-3})^{0.5}$ [24,30]. Therefore THF and acetone have the highest affinity to PEEK and should be more difficult to remove from the pores, resulting on them being more open. This seems to be the case since these membranes presented the highest MWCO. However, when considering IPA, which has higher affinity to PEEK than MeOH and should be therefore more difficult to remove from the pores, the opposite is observed: the IPA-dried membrane is tighter than the MeOH one. Again it seems that the contribution of the solvent–polymer affinity factor is not the primary driver and that other factors are dominant during the membrane drying.

It should be also noted that none of the parameters in Eq. (3) is independent of the temperature. In fact both the solvent surface tension and the tensile modulus decrease with the increase of the drying temperature [31,32]. The rate of this decrease in both terms of Eq. (3) may actually change the inequality for a given pore radius, and thus alter the degree of pore collapse. This effect may also contribute to the fact that for temperatures between 40 °C and 80 °C the rejection values were quite similar and they did not follow a specific order. It has been shown however that close to the glass-transition temperature PEEK undergoes a sharp decline in the tensile strength (Fig. 15 Appendix). Therefore between 120 °C and 140 °C the effect of the surface tension should be more pronounced. In other words, a fair comparison between different drying solvents can be made for a drying temperature of 120 °C, where all solvents were presumably completely evaporated and pore collapse was predominantly due to the surface tension effect. Such comparison is shown in Fig. 10. As expected, membranes dried from water had a higher extent of pore collapse when compared with membranes dried from other solvents. This is in accordance with predictions from Brown's theory, but does not explain the results obtained for the other solvents.

4. Modelling the post-phase inversion drying process of PEEK nanofiltration membranes

As mentioned before, the drying of PEEK membranes is a very complex phenomenon involving interactions between the solvent and the polymeric membrane as well as mass and heat transfer

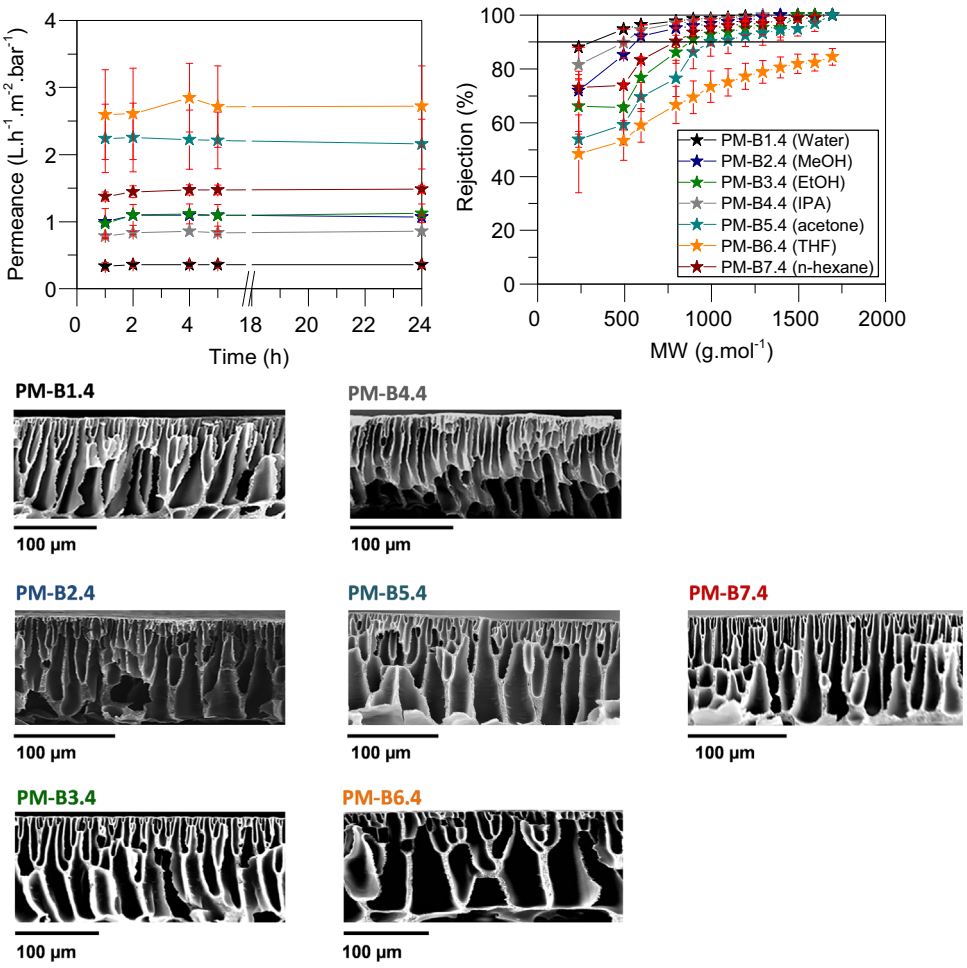

Fig. 10. Top left: Permeance values (L h^{-1} m^{-2} bar^{-1}) over a period of 24 h for the different membranes under study. Top right: Rejection values of the different PEEK membranes under study as a function of the molecular weight (M_W, g mol^{-1}) of different polystyrenes after 24 h. Membranes PM-B1.4, PM-B2.4, PM-B3.4, PM-B4.4, PM-B5.4, PM-B6.4 and PM-B7.4 were dried at 120 °C prior to their insertion in the cross-flow cells from water, MeOH, EtOH, IPA, acetone, THF and n-hexane, respectively. The membranes were filtered with a solution of THF and PS (1 g L^{-1}). The flow-rate, temperature and pressure were set at 100 L h^{-1}, 30 °C and 30 bar, respectively. The red bars represent the standard deviation of the mean. The membranes dried from water, MeOH, EtOH, IPA, acetone, THF and n-hexane at 120 °C are significantly different ($p \leq 0.05$, *F*-test). Bottom: Cross-section SEM images (magnification 300 ×) of the different membranes under study: PM-B1.4, PM-B2.4, PM-B3.4, PM-B4.4, PM-B5.4, PM-B6.4 and PM-B7.4. (For interpretation of the references to color in this figure legend, the reader is referred to the web version of this article.)

mechanisms combined with capillary forces. To date a satisfying phenomenological theory to describe such phenomenon has not been developed.

In order to understand which are the most important solvent properties that affect the drying process, a genetic algorithm was used in this research work to correlate solvent properties with membrane performance (the solvent permeance and the α-methyl styrene dimer flux were used as performance descriptors). The "weight" of each property was computed in order to assess the relevance of the parameters. The membrane performance at 120 °C was chosen for each solvent, since this was characterised by a more pronounced variation of permeance and MWCO (see Fig. 10). The solvent properties were obtained from literature for 20 °C and no correction of the solvent properties with temperature was implemented. As not all the properties can be easily correlated with temperature, the choice of using all the properties at 20 °C was made to avoid introduction of further sources of error.

The solvent properties were chosen in order to account for heat transfer contribution (vapour pressure), mass transfer contribution (viscosity), capillary forces (surface tension), steric effects (molar volume) and interactions between solvent and polymeric material (Hansen solubility parameter and polarity parameter). Initially, a linear model was used to describe the experimental flux data, with and without constant factor (Eq. (7)). In order to have an overdetermined system, a total of nine solvents was used. In addition to the seven solvents reported in the previous sections, acetonitrile and n-heptane were introduced. Properties and performance results for all these solvents can be found in Table 8 (Appendix). The regression system is overdetermined, as seven model parameters are regressed from performance data of nine different solvents. In order to evaluate the regression performance of the algorithm certain statistical measures have been proposed. The main measures used in literature are the Mean Absolute Error (MAE), the Mean Absolute Percentage Error (MAPE), the Mean Square Error (MSE) and the Root Mean Square Error (RMSE) [33]. In this work we chose the MAPE (defined below, Eq. (8)) as a measure of the error.

$$Y_{model}^{Sj} = b_0 + \sum_{i=1}^{n} b_i X_i^{Sj} \tag{7}$$

$$\text{MAPE}\ (\%) = \frac{1}{n}\sum_{j=1}^{n}\left|\frac{Y_{exp}^{Sj} - Y_{model}^{Sj}}{Y_{exp}^{Sj}}\right| \times 100 \tag{8}$$

where Y_{model}^{Sj} is the model prediction for performance (solute flux or permeance) in respect to a given solvent j (j=1,…,9), X_i^{Sj} is the solvent property (i=1,…,6), b_0 is the constant factor, b_i is the

Table 4
Solute flux model coefficients associated with solvent properties.

Solvent property	Coefficient associated with solvent property (b_i)				
	Symbol	Solute flux		Permeance	
		Linear model with constant factor	Linear model without constant factor	Linear model with constant factor	Linear model without constant factor
Constant factor	b_0	123	Not applicable	16.8	Not applicable
Vapour pressure (X_1)	b_1	-3.86×10^{-1}	-3.95×10^{-1}	7.47×10^{-3}	3.04×10^{-3}
Surface tension (X_2)	b_2	7.31×10^{-1}	2.08	-6.88×10^{-2}	1.16×10^{-1}
Hansen solubility parameter (X_3)	b_3	−5.00	−12.7	3.55×10^{-1}	-7.14×10^{-1}
Polarity parameter (X_4)	b_4	-4.89×10^{-1}	3.06	-3.16×10^{-1}	1.71×10^{-1}
Molar volume (X_5)	b_5	-4.76×10^{-1}	-1.45×10^{-1}	-5.18×10^{-2}	4.10×10^{-1}
Viscosity (X_6)	b_6	−7.48	−14.4	3.72×10^{-1}	-5.79×10^{-1}

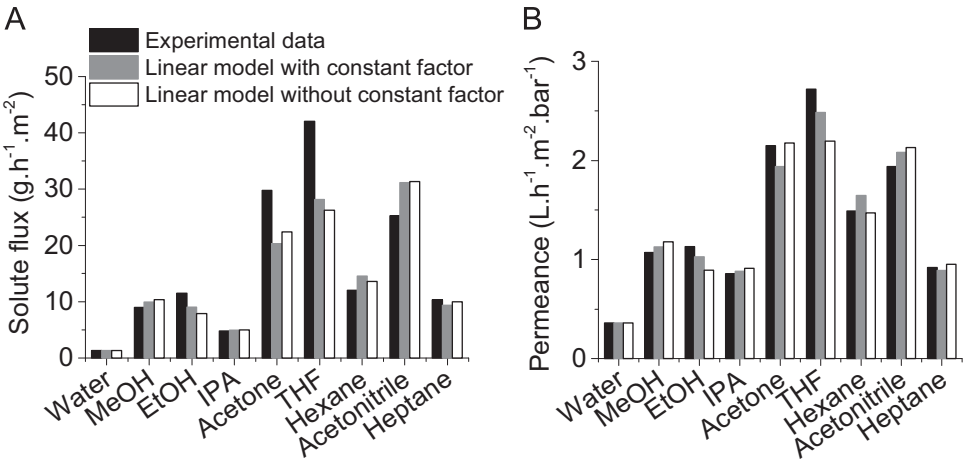

Fig. 11. A: Experimental data for solute flux and prediction of solute flux values using linear model with and without constant factor. B: Experimental data for permeance and prediction of permeance values using linear model with and without constant factor.

coefficient associated with each X_i^{Sj} (model coefficient), n is the number of solvents studied and Y_{exp}^{Sj} is the experimental result for performance (solute flux or permeance) in respect to a given solvent j (j=1,…,9). In this work, the values of MAPE correspond to the sum of the contribution from permeance and solute flux, i.e., $MAPE_{Total} = MAPE_{permeance} + MAPE_{rejection}$. The coefficients associated with solvent property (b_i) for both solute flux and permeance are presented in Table 4 and the experimental data and model fitting are presented in Fig. 11.

The MAPE values for linear model with and without constant factor were 9.58% and 9.80% respectively. Based on this result, the linear model with constant factor showed the best fitting and it was chosen for assessing the parameter weight (%). The parameter weight (%) was calculated using the equation below and the results are shown in Table 5.

$$\text{Parameter weight (\%)} = \frac{\left|b_i X_i^{Sj}\right|}{\sum_{i=0}^{n}\left|b_i X_i^{Sj}\right|},\quad i = 0,\ \ldots,\ 9;\quad X_0^{Sj} = 1 \tag{9}$$

Table 5
Parameter weight (%) for both solute flux and permeance using the linear model with constant factor. The sign in brackets indicates if a given solvent property had a negative or positive effect on the overall response.

Solvent property	Parameter weight (%)	
	Solute flux	Permeance
Vapour pressure	1.91 (−)	0.19 (+)
Surface tension	7.32 (+)	4.54 (−)
Hansen solubility parameter	21.80 (−)	10.14 (+)
Polarity parameter	8.02 (−)	33.89 (−)
Molar volume	13.57 (−)	9.85 (−)
Viscosity	1.96 (−)	0.64 (+)
Constant factor	45.41 (+)	40.70 (+)

The most important parameters are polarity, Hansen solubility parameter and molar volume for both permeance and solute flux. For the solute flux model, all these parameters had a negative effect whereas for the permeance model the Hansen solubilty parameter had a positive effect and both polarity and molar volume had a negative effect. Nevertheless, the constant factor showed higher importance for both models. By carrying on with the three most important parameters, it was possible to develop a linear model which accounts for single effects as well as interaction effects (Eq. (10)).

$$Y_{model}^{Sj} = b_0 + b_3X_3^{Sj} + b_4X_4^{Sj} + b_5X_5^{Sj} + c_1X_3^{Sj}X_4^{Sj} + c_2X_3^{Sj}X_5^{Sj} + c_3X_4^{Sj}X_5^{Sj} \tag{10}$$

c_i denotes coefficients associated with solvent property interactions. The coefficients associated with solvent property (b_i) or with solvent property interactions (c_i) for both solute flux and permeance are presented in Table 6 and the experimental data and model fitting are presented in Fig. 12.

The regression improved significantly with respect to the

Table 6
Solute flux model coefficients associated with solvent properties and solvent property interactions.

Solvent property/solvent property interaction	Coefficient associated with solvent property/ solvent property interaction (b_i or c_i)		
	Symbol	Solute flux	Permeance
Constant factor	b_0	473.7	30.4
Hansen solubility parameter (X_3)	b_3	-3.02×10^{1}	−2.02
Polarity parameter (X_4)	b_4	−6.44	-3.99×10^{-1}
Molar volume (X_5)	b_5	−1.76	-1.09×10^{-1}
$X_3 \times X_4$	c_1	4.05×10^{-1}	2.76×10^{-2}
$X_3 \times X_5$	c_2	2.83×10^{-1}	1.28×10^{-2}
$X_4 \times X_5$	c_3	-4.02×10^{-2}	-1.42×10^{-3}

model that accounted for single effects only. The MAPE value for linear model with interactions was 1.41% which was much lower than the one obtained for the linear models without property interactions. This result showed that taking into account the three most important parameters and their interactions improves the fitting, suggesting that the properties were not completely independent of each other. The parameter weight/solvent property interaction (%) was calculated using Eq. (9) and the results are shown in Table 7.

Polarity and Hansen solubility parameter were still the most important parameters but molar volume was surpassed by the interaction between the Hansen solubility parameter and polarity and by the interaction between Hansen solubility parameter and molar volume. The signs of the parameters – which indicates positive or negative effect – were the same for both solute flux and permeance (sovent flux). This means that both solute and solvent flux were affected in the same way by the solvent properties/solvent property interaction. These results showed again how important the interactions between solvent properties were in terms of model fitting.

Overall polymer drying is a very complex and not well understood phenomena. Further extensive investigation is required to elucidate and gain a better control over the PEEK nanofiltration membrane properties. We are confident that the research on this interesting, exceptionally stable material in the area of OSN will continue, and this work presents a first step in this direction.

Table 7
Parameter weight (%) for both solute flux and permeance using the linear model with interactions. The sign in brackets indicates if a given solvent property/ solvent property interaction had a negative or positive effect on the overall response.

Solvent property/ solvent property interaction	Parameter weight/solvent property interaction (%)	
	Solute flux	Permeance
Constant factor (b_0)	26.06 (+)	27.80 (+)
Hansen solubility parameter (X_3)	19.38 (−)	15.38 (−)
Polarity parameter (X_4)	15.62 (−)	15.99 (−)
Molar volume (X_5)	7.64 (−)	7.92 (−)
$X_3 \times X_4$	12.40 (+)	13.79 (+)
$X_3 \times X_5$	12.00 (+)	9.09 (+)
$X_4 \times X_5$	6.91 (−)	4.09 (−)

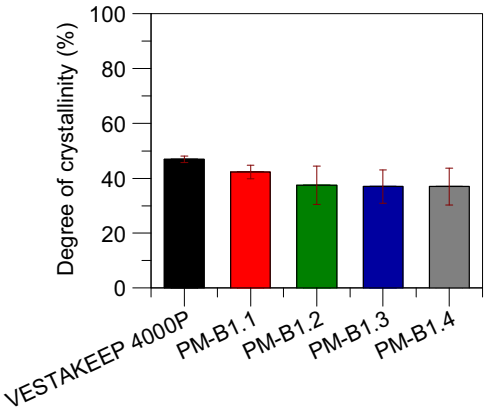

Fig. 13. Degree of crystallinity (%) obtained from DSC (2.3.3) for VESTAKEEP 4000P and membranes PM-B dried from water at different temperatures: PM-B1.1, PM-B1.2, PM-B1.3 and PM-B1.4. The error bars represent the standard deviation from two sequential heating cycles.

5. Conclusions

The post-fabrication drying process of PEEK membranes was found to be the reason for variation in the separation performance from the ultra to nanofiltration range. Two factors were investigated in an attempt to manipulate membrane MWCO: the concentration of polymer in the dope solution and the solvent filling the pores prior to drying. When varying the polymer dope concentration from 8 wt% to 12 wt% a shift from more open membranes (8 wt%) to tighter membranes (10 wt% and 12 wt%)

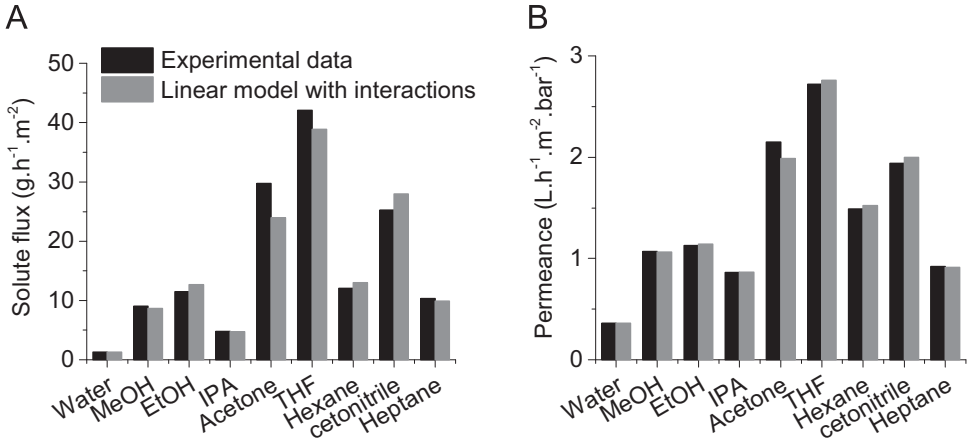

Fig. 12. A: Experimental data for solute flux and prediction of solute flux values using linear model with interactions. B: Experimental data for permeance and prediction of permeance values using linear model with interactions.

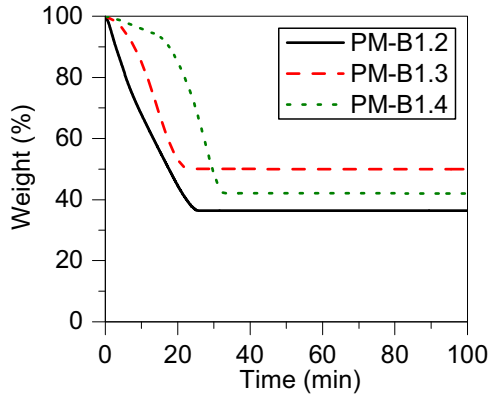

Fig. 14. Weight loss (%) as a function of time (min) obtained from TGA analysis for membranes PM-B dried at different temperatures (40 °C, 80 °C and 120 °C).

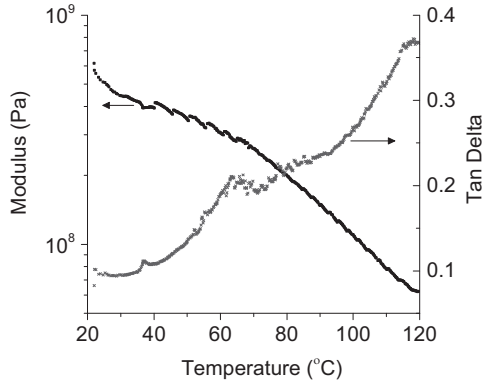

Fig. 15. Values of dynamic modulus (stiffness, Pa) and mechanical damping (tan delta) for membrane PM-B 12 wt%. The membrane was inserted while water "wet" at a heating rate of 2 K min^{-1}. The tests were carried out at 1 Hz with a displacement of 0.05 mm.

was observed. A parallel between dope solution viscosity and membrane performance was drawn in order to explain the difference in performance for different polymer concentrations: the higher the viscosity the tighter the membranes produced. The type of solvent filling the membrane pores prior to drying had a pronounced effect on the separation performance. It was possible to vary the MWCO from 295 g mol^{-1} to 1400 g mol^{-1} (in terms of nanofiltration range). Another parameter studied for both factors (polymer concentration and solvent filling prior to drying) was the effect of drying temperature. For membranes dried from water the effect of drying temperature was negligible whereas for membranes dried from other solvents the effect was more pronounced (e.g. acetone and THF). In summary, by increasing the temperature from 20 °C to 120 °C it was possible to further manipulate the MWCO when drying from the same solvent. In order to set some guidance (and understanding) for a phenomenological study of membrane drying a statistical analysis of the presented data was performed in order to assess the relevant solvent properties involved. The Hansen solubility parameter, polarity and their interactions with molar volume were found to be the most important parameters influencing membrane MWCO. Nevertheless, this is just the beginning of a very complex phenomenon that needs to be further pursued in order to be fully understood.

Author contributions

The manuscript was written through contributions of all authors. All authors have given approval to the final version of the manuscript.

Acknowledgements

This work was funded by the Novartis Pharma AG, Massachusetts Institute of Technology, USA sub-award Agreement no. 5710002924. The authors would like to acknowledge EPSRC, United Kingdom for the financial support under the Project EP/J014974/1 entitled Molecular Builders: Constructing Nanoporous Materials.

Appendix

See Figs. 13–15 and Table 8.

Nomenclature

p or Δp	applied pressure (Pa or bar)
A	area (m^2)
F_c	capillary forces (N)
C	concentration (mol m^{-3})
L_P	permeance (L h^{-1} m^{-2} bar^{-1})
R_i	rejection of solute i ((dimensionless) or %)
E	tensile modulus of the polymer material (N m^{-2})
t	time (s or h)
μ	viscosity (Pa s)
J	volumetric flux (L h^{-1} m^{-2})

Table 8
Properties of the solvents used for the solvent exchange: vapour pressure (kPa), surface tension (mN m^{-1}), Hansen solubility parameter (cal $cm^{-3})^{0.5}$, polarity parameter (kcal mol^{-1}), molar volume (cm^3 mol^{-1}) and viscosity (cP). All properties listed were obtained from [34] at 20 °C and 1 bar. In addition, rejection values (%) for the dimer (M_W=236 g mol^{-1}) and permeance values (L h^{-1} m^{-2} bar^{-1}) for PEEK membranes 12 wt% dried at 120 °C from the corresponding solvent, and used for the modelling, are presented.

	Vapour pressure (kPa)	Surface tension (mN m^{-1})	Hansen solubility parameter (cal $cm^{-3})^{0.5}$	Polarity parameter (kcal mol^{-1})	Molar volume (cm^3 mol^{-1})	Viscosity (cP)	Rejection (%)	Permeance (L h^{-1} m^{-2} bar^{-1})
Water	2.33	72.75	25.5	63.1	18	1	88.05	0.36
MeOH	16.933	22.6	14.5	55.4	40.6	0.6	71.9268	1.07
EtOH	5.9466	22.3	13.4	51.9	58.6	1.08	66.13	1.13
IPA	4.1	21.7	11.5	48.4	76.9	2	81.5211	0.86
Acetone	30.8	23.3	10	42.2	73.8	0.33	53.85	2.15
THF	21.6	26.4	9.1	37.4	81.9	0.46	48.44	2.72
Hexane	20.17	18.4	6.9	31	131.4	0.31	73.06	1.49
Acetonitrile	9.6	29.1	11.9	45.6	52.9	0.38	56.57	1.94
Heptane	6.093	19.3	7.5	31.1	147	0.41	62.69	0.92

Greek symbols

θ	contact angle between the liquid and the membrane material (°)
Φ_i	[artition coefficient (dimensionless)
ε	surface porosity (dimensionless)
γ	surface tension of the gas/liquid interface ($N\,m^{-2}$)

Subscripts

i	

References

[1] L. Peeva, J. da Silva Burgal, S. Vartak, A.G. Livingston, Experimental strategies for increasing the catalyst turnover number in a continuous Heck coupling reaction, J. Catal. 306 (0) (2013) 190–201.

[2] H. Strathmann, K. Kock, The formation mechanism of phase inversion membranes, Desalination 21 (3) (1977) 241–255.

[3] Y.H. See-Toh, M. Silva, A. Livingston, Controlling molecular weight cut-off curves for highly solvent stable organic solvent nanofiltration (OSN) membranes, J. Membr. Sci. 324 (1–2) (2008) 220–232.

[4] I. Soroko, A. Livingston, Impact of TiO2 nanoparticles on morphology and performance of crosslinked polyimide organic solvent nanofiltration (OSN) membranes, J. Membr. Sci. 343 (1–2) (2009) 189–198.

[5] P. Vandezande, L.E.M. Gevers, I.F.J. Vankelecom, Solvent resistant nanofiltration: separating on a molecular level, Chem. Soc. Rev. 37 (2) (2008) 365–405.

[6] M. Bulut, L.E.M. Gevers, J.S. Paul, I.F.J. Vankelecom, P.A. Jacobs, Directed development of high-performance membranes via high-throughput and combinatorial strategies, J. Comb. Chem. 8 (2) (2006) 168–173.

[7] Y.H. See-Toh, F.C. Ferreira, A.G. Livingston, The influence of membrane formation parameters on the functional performance of organic solvent nanofiltration membranes, J. Membr. Sci. 299 (1–2) (2007) 236–250.

[8] T. Shimoda, H. Hachiya, Process for preparing a polyether ether ketone membrane, 5,997,741, 1999, US Patent 5,997,741, 08/836,034.

[9] I.F.J. Vankelecom, K.D. Smet, L.E.M. Gevers, P.A. Jacobs, Nanofiltration membrane materials and preparation, in: A.I. Schäfer, A.G. Fane, T.D. Waite (Eds.), Nanofiltration – Principles and Applications, Elsevier, Oxford, 2006, pp. 33–42.

[10] I. Soroko, M. Makowski, F. Spill, A. Livingston, The effect of membrane formation parameters on performance of polyimide membranes for organic solvent nanofiltration (OSN). Part B: Analysis of evaporation step and the role of a co-solvent, J. Membr. Sci. 381 (1–2) (2011) 163–171.

[11] T.-H. Young, J.-H. Huang, W.-Y. Chuang, Effect of evaporation temperature on the formation of particulate membranes from crystalline polymers by dry-cast process, Eur. Polym. J. 38 (1) (2002) 63–72.

[12] P.J. Rae, E.N. Brown, E.B. Orler, The mechanical properties of poly(ether-ether-ketone) (PEEK) with emphasis on the large compressive strain response, Polymer 48 (2) (2007) 598–615.

[13] H.I. Kim, S.S. Kim, Plasma treatment of polypropylene and polysulfone supports for thin film composite reverse osmosis membrane, J. Membr. Sci. 286 (1–2) (2006) 193–201.

[14] M.A.M. Beerlage, Polyimide Ultrafiltration Membranes for Non-aqueous Systems, 1994.

[15] P. Manos, Solvent exchange drying of membranes for gas separation, US Patent 4120098 A, 1978.

[16] I.-C. Kim, H.-G. Yun, K.-H. Lee, Preparation of asymmetric polyacrylonitrile membrane with small pore size by phase inversion and post-treatment process, J. Membr. Sci. 199 (1–2) (2002) 75–84.

[17] P. Manos, Gas separation membrane drying with water replacement liquid, US Patent 4080744 A, US05/698,697, 1978.

[18] W. MacDonald, C.-Y. Pan, Method for drying water-wet membranes, US Patent 1974 3,842,515, 1974.

[19] W.M. King, M.-W. Tang, C.G. Wensley, Air dried cellulose acetate membranes, US Patent 4855048 A, 1989.

[20] G.L. Brown, Formation of films from polymer dispersions, J. Polym. Sci. 22 (102) (1956) 423–434.

[21] P. Manos, Membrane drying process, US Patent 4080743 A, 1978.

[22] J. da Silva Burgal, L.G. Peeva, S. Kumbharkar, A. Livingston, Organic solvent resistant poly(ether-ether-ketone) nanofiltration membranes, J. Membr. Sci. 479 (0) (2015) 105–116.

[23] D.J. Blundell, B.N. Osborn, The morphology of poly(aryl-ether-ether-ketone), Polymer 24 (8) (1983) 953–958.

[24] Y.H. See Toh, F.W. Lim, A.G. Livingston, Polymeric membranes for nanofiltration in polar aprotic solvents, J. Membr. Sci. 301 (1–2) (2007) 3–10.

[25] I.M. Smallwood, Handbook of Organic Solvent Properties, Elsevier, Amsterdam, 1996.

[26] L.E.M. Gevers, S. Aldea, I.F.J. Vankelecom, P.A. Jacobs, Optimisation of a lab-scale method for preparation of composite membranes with a filled dense top-layer, J. Membr. Sci. 281 (1–2) (2006) 741–746.

[27] H. Matsuyama, M.-m Kim, D.R. Lloyd, Effect of extraction and drying on the structure of microporous polyethylene membranes prepared via thermally induced phase separation, J. Membr. Sci. 204 (1–2) (2002) 413–419.

[28] X. Jie, Y. Cao, J.-J. Qin, J. Liu, Q. Yuan, Influence of drying method on morphology and properties of asymmetric cellulose hollow fiber membrane, J. Membr. Sci. 246 (2) (2005) 157–165.

[29] H. Matsuyama, A. Yamamoto, H. Yano, T. Maki, M. Teramoto, K. Mishima, K. Matsuyama, Effect of organic solvents on membrane formation by phase separation with supercritical CO_2, J. Membr. Sci. 204 (1–2) (2002) 81–87.

[30] J. Scheirs, Surface-tension and solubility-parameter effects, in: Compositional and Failure Analysis of Polymers: A Practical Approach, Wlley, 2000.

[31] E.W. Flick, Industrial Solvents Handbook, 5th ed., William Andrew Publishing/Noyes, New York, 1998.

[32] VICTREX Material Properties Guide. http://www.victrex.com/docs/literature-docs/Victrex_Material%20Properties%20Guide%20%20%203_7_US.pdf.

[33] E.S. Gardner, Forecasting: methods and applications (second edition), Makridakis, S., Wheelwright, S.C. and McGee, V.E., New York: Wiley, 1983. In Journal of Forecasting, John Wiley & Sons, Ltd.: 1984; Vol. 3, pp 457–460.

[34] G. Wypych, Knovel Solvents – A Properties Database, ChemTec Publishing, 2008.